Integrated Non-model-based Adaptive Optimal Control of SCR and APH Systems at Cayuga Unit 1

Eugenio Schuster[1], Carlos E. Romero, Zheng Yao
Energy Research Center, Lehigh University,
117 ATLSS Drive, Bethlehem, PA 18015, USA

Fengqi Si
School of Energy and Environment, Southeast University
Si Pai Lou No. 2, Nanjing 210096, PR China

Robert L. Morey and Jacob A. Peter
AES Cayuga, LLC
228 Cayuga Drive, Lansing, NY 14882, USA

Barry N. Liebowitz
New York State Energy Research and Development Authority
17 Columbia Circle, Albany, NY 12203, USA

ABSTRACT

AES Cayuga Unit 1 is a 160 MW unit, equipped with a low-NO_x firing system and an anhydrous ammonia, $TiO_2/V_2O_5/WO_3$ Selective Catalytic Reduction (SCR) system for NO_x emissions control. A Breen Energy Solutions ammonium bisulfate (ABS) probe was retrofit to the SCR to monitor ABS formation in real-time. A recently proposed control system upgrade includes a control strategy provision for the air preheater (APH) bypass damper. Such control strategy regulates the ABS deposition location by manipulating the average cold end APH temperature with the ultimate goal of minimizing APH plugging (ABS concentration). Extremum Seeking (ES) is an adaptive control method, usable for optimally tuning both set-points and controller parameters in regulation problems. It is a non-model based method of adaptive optimal control, and, as such, it solves, in a rigorous and practical way, some of the same problems as artificial neural network (ANN) and other intelligent control techniques. ES is applicable in situations where there is a nonlinearity in the control problem, and the nonlinearity has a local minimum or a maximum. The nonlinearity may be in the plant, as a physical nonlinearity, possibly manifesting itself through an equilibrium map. Hence, one can use ES for on-line optimal tuning of a set point to achieve an optimal value of the output. An ES controller is proposed to regulate the NH_3 flow to the SCR system and the APH bypass damper opening in order to optimally control in real time and in a coordinated fashion both continuous emissions monitoring (CEM) NO_x and ABS deposition location within the APH, avoiding NH_3 slip and minimizing APH heat rate penalty. The effectiveness of the ES adaptive controller in keeping the system at an optimal operation point in presence of input disturbances and system changes (unit load, coal quality, firing system maintenance condition, SCR aging, etc.) is demonstrated through simulations.

Keywords: Real-time Optimal Control, Integrated SCR/APH Control.

---

[1] *Corresponding Author: Tel: 610-758-5253, Fax: 610-758-6224, E-mail: schuster@lehigh.edu*

1. Introduction

Utilities have a variety of methods for reducing nitrogen oxide (NOx) emissions from existing boilers, and achieving compliance with strict federal and state regulations in the US for NOx. These methods range from low-NOx burner retrofitting to using post-combustion controls, such as selective catalytic reduction (SCR) systems. SCR is generally the most expensive method for NOx emissions control, but is also the most effective. However, stringent state implementation plan (SIP) Call NOx mandates, have motivated widespread planning for retrofitting approximately 100 GW of coal-fired capacity in the US (Cichanowicz, 2002). NOx SIP Call requirements provide incentive for designing and operating SCR process equipment to consistently achieve 90% NOx removal, in most of the cases, year-round. SCR systems are commonly designed to work with liquid anhydrous ammonia (NH3) and aqueous NH3, where the NH3 reacts with the NOx in the flue gas, reducing the oxides to molecular nitrogen and water. Although, the SCR catalyzed chemical reactions are very efficient, a small portion of the reagent does not react and leaves the reactor as ‘‘NH3 slip.” Slippage problems increase as the SCR catalyst ages and the catalyst surface become masked or plugged with fly ash. When this happens, the required NH3 slip increases, resulting in boiler air preheater (APH) fouling by ammonium/sulfur salts. Controlling and mitigating APH fouling is imperative in coal-fired boilers, since that air handling limitations and corrosion preclude continued operation of the unit, requiring unit shutdown for APH cleaning, with the associated lost in unit availability and financial losses.

During the last few years, the ever-increasing demand for cost-efficient power generation and stringer environmental regulation has motivated implementation of process optimization strategies in coal-fired power generations. Given that coal is an important element in the energy source portfolio in the US, process optimization for stack emissions reductions and efficiency improvements in coal-fired boilers plays an important role in minimizing operational & maintenance (O&M) costs, and maximizing performance and unit availability. One area that has received significant attention is tuning and optimization of the combustion process for NOx emissions and unit thermal performance improvement. There is a large list of reported experiences where combustion optimization has proved to be an effective method to reduce NOx emissions, while mitigating its impact on the net unit heat rate (Romero, 2000). With the growing population of SCR systems already retrofitted and projected to be retrofitted in the US, an extension of such optimization techniques to the combined SCR/APH systems is worth exploring.

AES Cayuga Unit 1 is a 160 MW unit, equipped with a low-NO_x firing system and an anhydrous ammonia, $TiO_2/V_2O_5/WO_3$ Selective Catalytic Reduction (SCR) system for NO_x emissions control. A Breen Energy Solutions ammonium bisulfate (ABS) probe was retrofit to the SCR to monitor ABS formation in real-time. A recently proposed control system upgrade includes a control strategy provision for the air preheater (APH) bypass damper. Such control strategy regulates the ABS deposition location by manipulating the average cold end APH temperature with the ultimate goal of minimizing APH plugging (ABS concentration). A real-time, adaptive, extremum-seeking (ES) controller (Ariyur, 2003) is proposed in this paper to regulate the NH_3 flow to the SCR system and the APH bypass damper opening in order to optimally control in real time and in a coordinated fashion both continuous emissions monitoring (CEM) NO_x and ABS deposition location within the APH, avoiding NH_3 slip and minimizing APH heat rate penalty.

2. System Configuration

We consider the system shown in Fig. 1 composed by the Selective Catalytic Reduction (SCR) System and the Air Preheater (APH). The regulation of some of the boiler conditions (O_2, SOFA, burner tilt, SOFA tilt, coal flow, etc.), which is not the focus of this work, determines the NO_x level at the SCR inlet. The adopted control strategy consists in: i- regulating NH_3 flow to control stack or continuous emissions monitoring (CEM) NO_x, ii- regulating the APH bypass damper to control ammonium bisulfate (ABS) deposition depth within the APH. Since the ABS deposition depth is also affected by the NH3 flow, an approach for integrated control of SCR and APH is discussed.

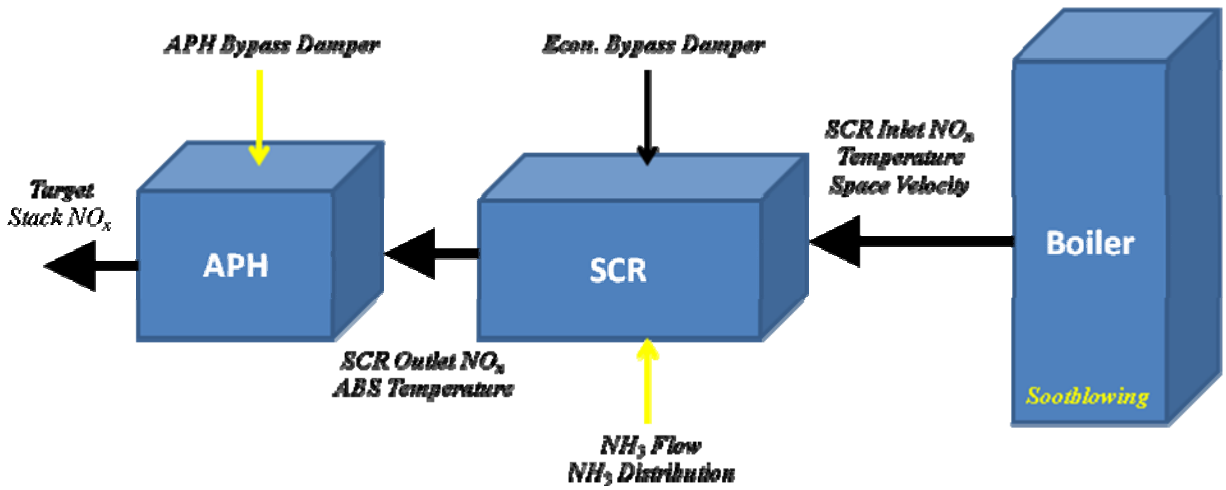

Fig. 1: System configuration.

2.1 SCR System

2.1.1 SCR Control

A typical SCR control system usually provided by manufacturers is shown in Fig. 2. The objective of the feedback control loop is to regulate the efficiency of the SCR system at a predefined value given by η_{SCR}. The injection of NH3 is dictated by this feedback loop but also by a feedforward controller, which makes the feedforward component of the NH3 flow just proportional to *NOx_in*. Although this scheme guarantees a specific efficiency, it cannot guarantee a specific value of CEM NOx.

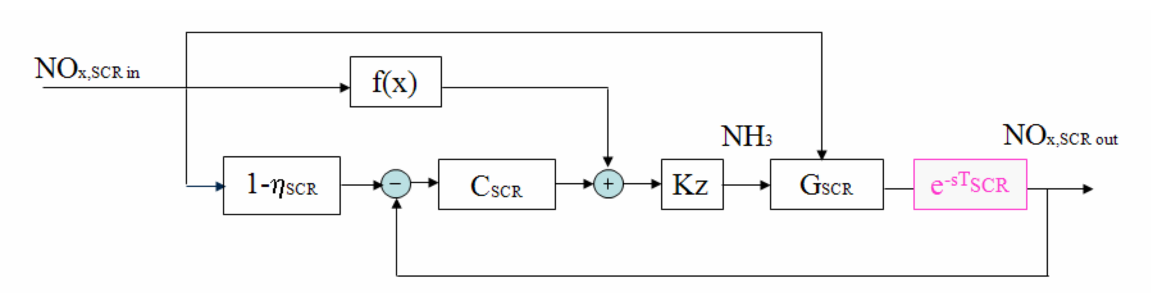

Fig. 2: SCR manufacturer's original control architecture.

By exploiting the availability of the continuous emissions monitoring system, it is possible to propose a different control approach where the ultimate goal is the regulation of the *NOx_CEM* level at a predefined value. The approach, illustrated in Fig. 3, also combines both feedforward and feedback loops.

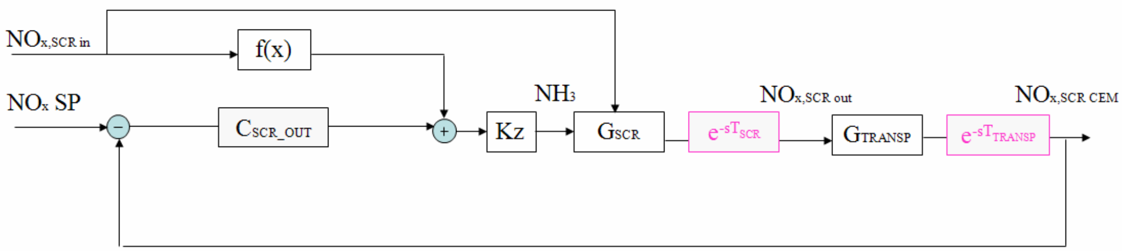

Fig. 3: SCR control architecture based CEM NOx.

Although this controller can in principle guarantee a specific level of *NOX_CEM*, the time delays both in the SCR system and in the transport channel (denoted in pink in both Fig. 2 and Fig. 3) can significantly affect the performance of the control approach. Since the NO_x signal from the plant CEM is used to regulate NH_3 flow, a pure time delay, associated with the measurement of this parameter, needs to be dealt with. There are several control methods to deal with time delays in feedback loops. However, most of them require a good knowledge, i.e., model, of the system, which is usually not the case in coal-based power plants. For this reason we propose a non-model-based approach consisting in a multi-loop PID approach combined with optimal tuning. Information on the rate of change of the NO_x at both the SCR inlet and the SCR otulet is incorporated into the NH_3 flow feedback controller in order to overcome the effect of the time delay and eliminate oscillations currently present in both the CEM NO_x and the NH_3 injection. In addition, not only positive but also negative feedback correction (bias) of the feedforward loop is allowed with the objective of eliminating NH_3 slip observed in the plant due to this control limitation. The proposed scheme is shown in Fig. 4, where the outer-loop controller $C_{SCR,OUT}$ is a Proportional-Integral-Derivative (PID) controller, the inner-loop controller $C_{SCR,IN}$ is a Proportional-Derivative (PD) controller, and the feedforward controller $C_{SCR,FEED}$ is a pure derivative (D) controller. The controller equations can be written as

$$C_{SCR\_OUT}(s) = K_{P,OUT} + K_{I,OUT}\frac{1}{s} + K_{D,OUT}s, \quad C_{SCR\_JN}(s) = K_{P,IN} + K_{D,IN}s, \quad C_{SCR\_FEED}(s) = K_{D,FEED}s \tag{1}$$

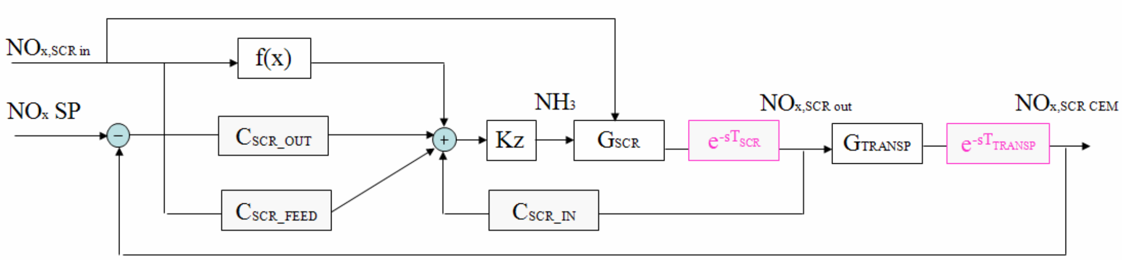

Fig. 4: Multi-loop SCR control architecture based on CEM NOx, SCR inlet NOx and SCR outlet NOx.

2.1.2 SCR Dynamic Model

In order to compare the different control approaches, and also to optimally tune the controller parameters to cope with the time delays, simulations were carried out using MATLAB SIMULINK@. For that purpose, a simplified model of the SCR system was created. The SIMULINK closed-loop system is illustrated in Fig. 5.

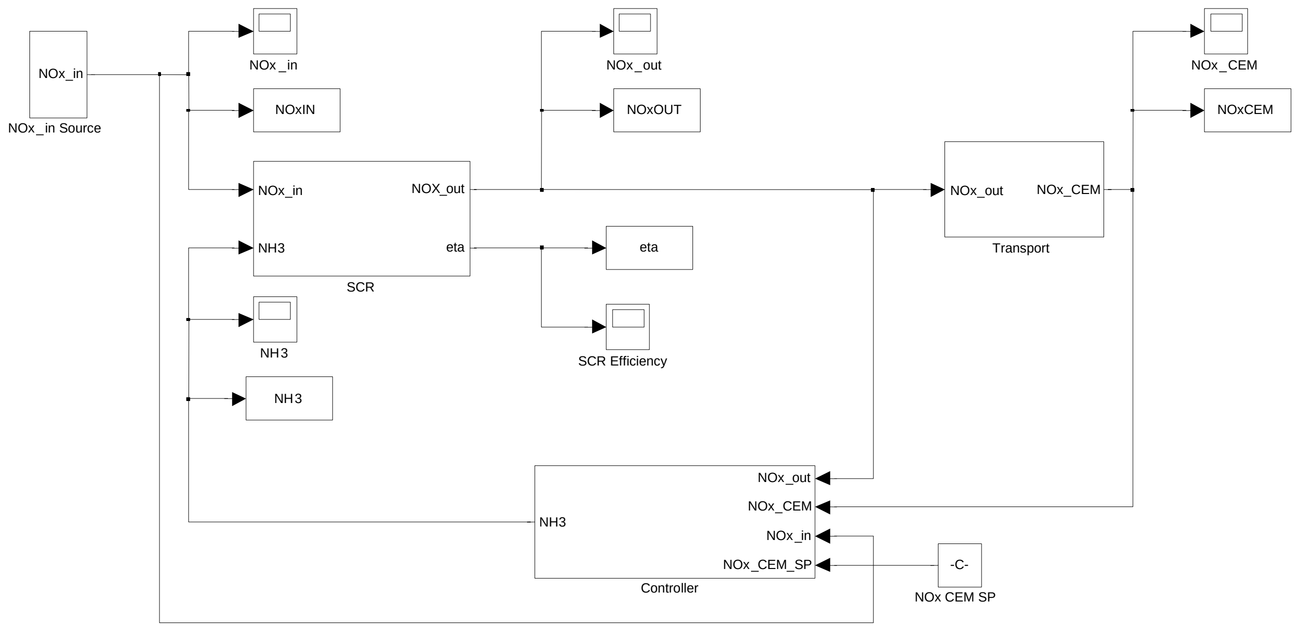

Fig. 5: Simulink SCR control configuration.

The SCR system is modeled as

$$NOx\_out = e^{-s\tau_{SCR,D}} \frac{1}{\tau_{SCR} s + 1} \eta(NH3/NOx\_in) NOx\_in, \tag{2}$$

where $\eta(NH3/NOx\_in)$, plotted in Fig. 6, was modeled using operational data obtained through parametric field tests at Cayuga Unit 1.

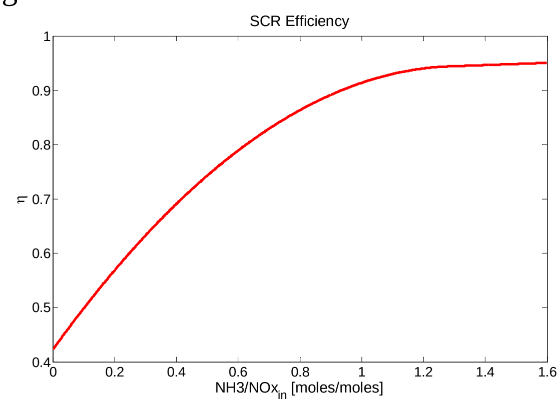

Fig. 6: SCR efficiency as a function of the NH3/NOx_in ratio.

The channel connecting the SCR and the stack was modeled as a transport line, where

$$NOx\_CEM = e^{-s\tau_{TRANSP,D}} \frac{1}{\tau_{TRANSP}s+1} NOx\_out. \quad \textbf{(3)}$$

The feedback component of the NH3 level injected into the SCR is contributed by three different controllers: a PID fed by the error between the *NOx_CEM* and its associated set-point, a PD controller fed by a measurement of the *NOx_out*, and a D controller fed by a measurement of the *NOx_in*. The gains of the controllers in (1) are optimally tuned following an extremum seeking approach. We are interested in tuning the controllers gains to minimize the tracking error, i.e., we define the to-be-minimized cost function as

$$J = \frac{1}{2}\int_{t_0}^{t_f} [NOx\_CEM(t) - NOx\_CEM\_setpoint(t)]^2\, dt \quad \textbf{(4)}$$

The chosen simulation parameters are $\tau_{SCR,D}$=30s, τ_{SCR}=10s, $\tau_{TRANSP,D}$=60s, τ_{TRANSP}=20s. The resulting optimal gains are $K_{P,OUT}$ =1.3182, $K_{I,OUT}$ =1.1563, $K_{D,OUT}$=1.0564, $K_{P,IN}$=2.9020, $K_{D,OUT}$=0.0170 and $K_{D,FEED}$=0.0572. Fig. 7 (d) shows the time response of the multi-loop system when *NOx_in* changes as illustrated in Fig. 7 (a). The feedback component of the NH3 injection is showed in Fig. 7 (b). As it can be noted from Fig. 7 (c), the SCR efficiency is not kept constant because the ultimate goal is the regulation of *NOx_CEM* at the desired set-point. Fig. 7 (d) shows that the controller successfully regulate the NOx level at the stack, rejecting the changes in *NOx_in*.

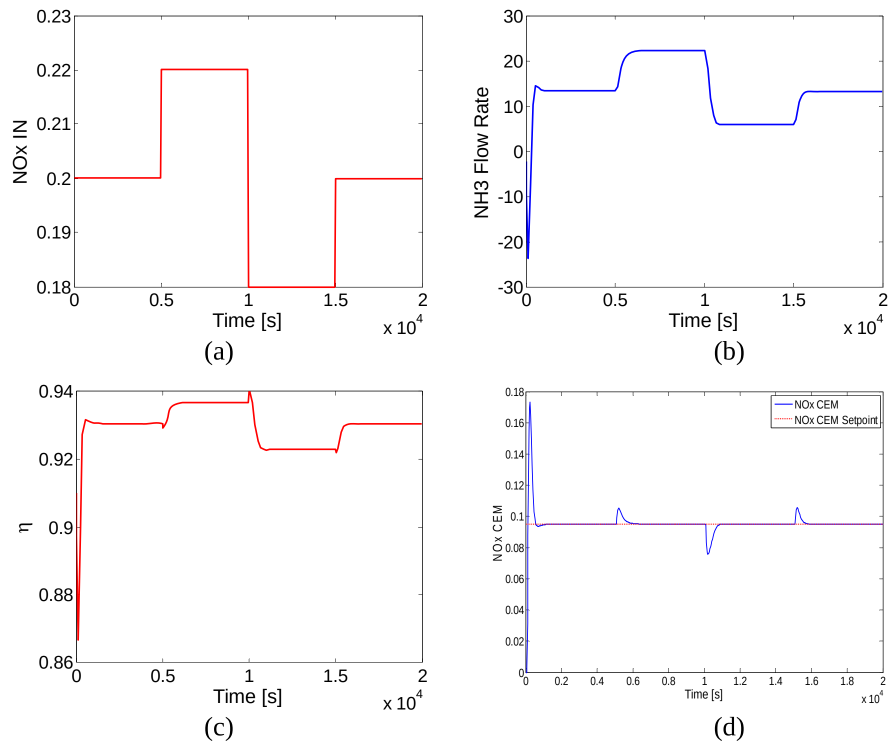

Fig. 7: Time response of the optimized multi-loop system.

2.2 Air Pre Heater (APH) System

2.2.1 APH Control

The control logic at Cayuga Unit 1 has been modified to include a scheme that incorporates the feedback measurements from Ammonium Bisulfate (ABS) fouling and Air Pre-Heater (APH) outlet temperature sensors and a control strategy provision for the air preheater (APH) bypass damper. The Breen Energy Solutions ammonium bisulfate (ABS) probe, retrofit to the SCR, together with temperature measurements allow for real-time estimation of the ABS deposition depth measured from the APH cold end. The ABS deposition location can be controlled by manipulating the average cold end APH temperature through the air preheater (APH) bypass damper with the ultimate goal of minimizing APH plugging (ABS concentration). Fig. 8 illustrates the APH control configuration. The deposition depth can be estimated through the function $D(x)$ from the ABS formation temperature, which is function of the NH3/NOx ratio, and the APH temperature, which can be controlled through the APH bypass damper (Si, in press). The PID control $K_{APH}*C_{APH}$ regulates the deposition depth to the desired set-point.

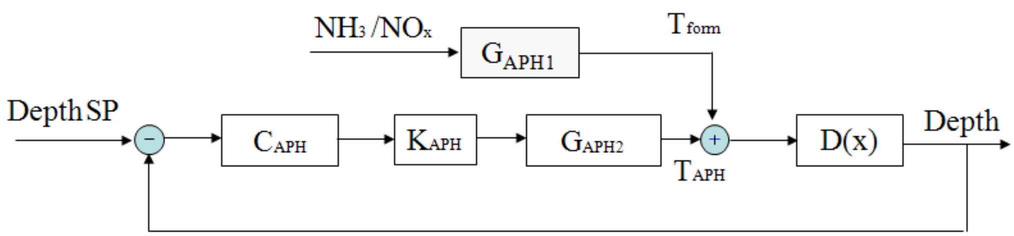

Fig. 8: APH control configuration.

2.2.2 APH Dynamic Model

In order to simulate the APH closed-loop system performance, simulations were carried out using MATLAB SIMULINK@. The simplified model for the APH dynamics is shown in Fig. 9. The ABS deposition depth is determined by both the formation temperature and the APH temperature. The response of the APH to the bypass damper is modeled as a simple first-order transfer function. The response of the formation temperature to the NH3/NOx_in ratio is modeled as a first-order transfer function in series with the nonlinear function in Fig. 10 (obtained by parametric test at Cayuga Unit 1).

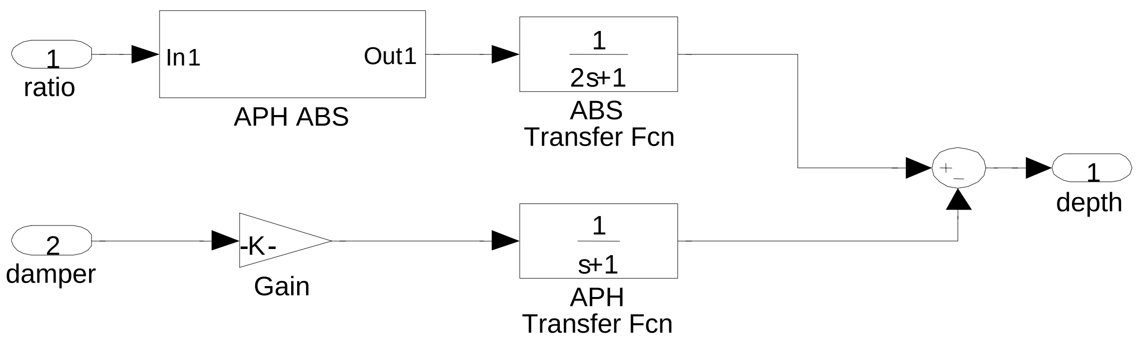

Fig. 9: Simplified APH model.

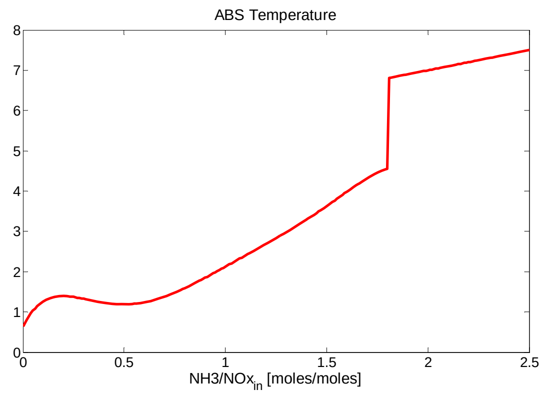

Fig. 10: ABS formation temperature as a function of NH3/NOx_in.

3. Integrated SCR/APH control

It is possible to note that the ABS deposition depth can be controlled not only by regulating the bypass damper but also by modulating the NH3/NOx_in. For a given *NOx_in*, a decrease in NH3 injection would result in a decrease of the NH3/NOx_in and in turns in the ABS temperature formation. A decrease of the ABS temperature formation would translate into a decrease of the deposition depth. Therefore, the decrease in NH3 injection could avoid the opening of the bypass damper and its associated heat rate penalty. Of course, a decrease in NH3 injection would result in an increase in *NOx_CEM*. There seems to be then a tradeoff between the NOx level at the stack and the HR penalty due to the opening of the bypass damper. However, if a small increase of *NOx_CEM* is tolerated, we can control the deposition depth by reducing the NH3 flow instead of by opening the bypass damper and avoid in this way a higher APH heat rate. Fig. 11 shows an ad hoc coordinated SCR and APH control scheme, where the block *E*(*x*) modifies the set-point for *NOx_CEM* as a function of the APH bypass damper opening, which is directly proportional to the APH heat rate penalty. The coordinator block *E*(*x*) will not modify the set-point for NOx_CEM as long as the APH bypass damper opening is smaller than a predefined threshold. When the APH bypass damper opening exceeds this threshold, the NOx_CEM set-point is modified proportionally to the APH bypass opening.

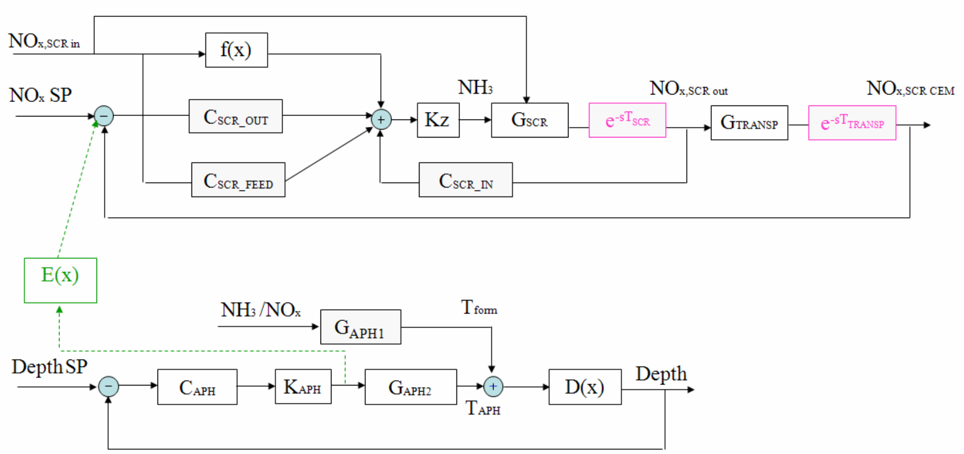

Fig. 11: Coordinated SCR and APH PID-based control.

Fig. 12 shows the effect of controlling the APH deposition depth via the manipulation of the NH3 injection by changing the set-point for *NOx_CEM*. We consider the case where *NOx_in* changes as shown in Fig. 12 (a). The blue line illustrates the case where no coordination is present. In this case the APS deposition depth is exclusively controlled by the APH bypass damper. Note from Fig. 12 (b) that the *NOx_CEM* is successfully regulated to the unmodified set-point shown in Fig. 12 (d). However, it is necessary in this case to inject a considerable amount of NH3 (see Fig. 12 (f)). This amount of NH3 will require also a considerable opening of the APH damper (see Fig. 12 (e)) to successfully regulate the APS deposition depth to a desired fixed set-point value (see Fig. 12 (c)). The green line illustrates the case where the threshold for coordination is zero. This means that the set-point for *NOx_CEM* will always be modified proportionally to the APH bypass damper. Fig. 12 (d) shows the modification of the *NOx_CEM* set-point to a higher value for which the NH3 injection can be significantly reduced (see Fig. 12 (f)) and consequently the APH bypass damper opening required to regulate the APH deposition depth is also significantly reduced (see Fig. 12 (e)), minimizing in this way the APH HR penalty at the expense of a higher level of NOx at the stack. Finally, the red line shows an intermediate case where the threshold for the coordinator block is set as 40% of the APH bypass damper opening. Once the damper opening exceeds this value the set-point for *NOx_CEM* is modified. Note how the slight increase of the set-point in Fig. 12 (d) allows reductions of both NH3 injection and APH bypass damper opening if compared to the uncoordinated case (blue line).

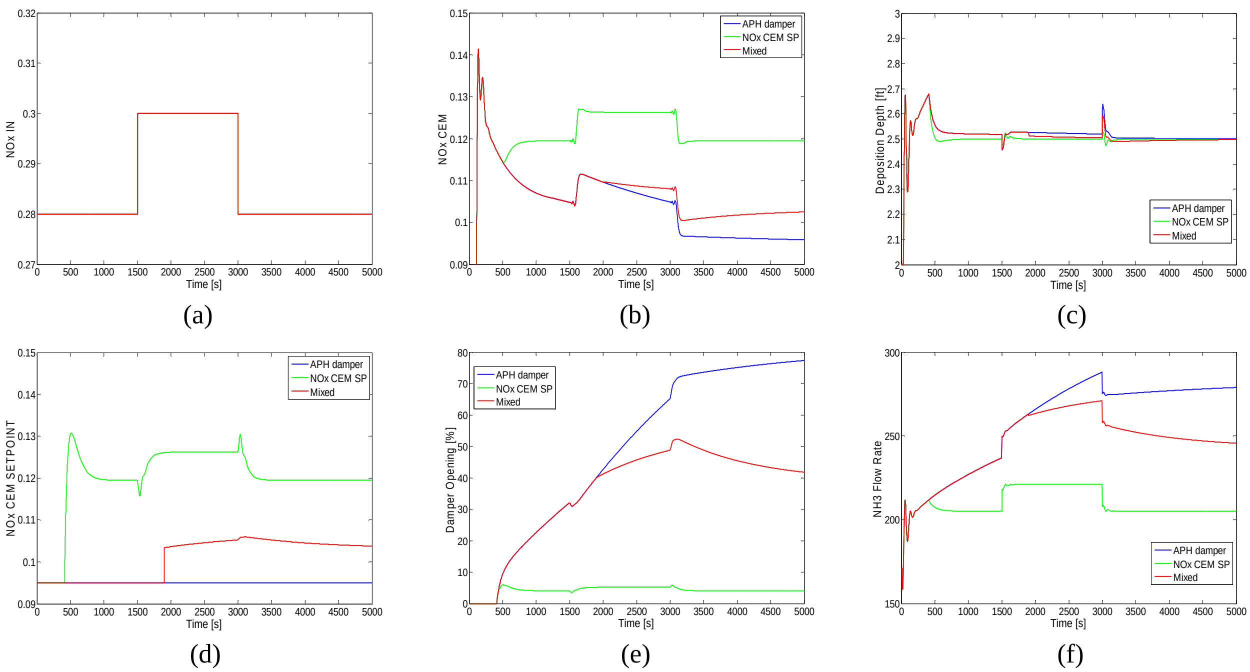

Fig 12: Effect of modification of NOx_CEM set-point.

4. Non-model-based Optimal Adaptive Control of SCR/APH System

Based on the results obtained in the previous section, we propose here an integrated, non-model-based, optimal, adaptive control strategy for the SCR/APH system based on Extremum Seeking (ES). The non-model-based ES controller is proposed to regulate the NH_3 flow to the SCR system and the APH bypass damper opening in order to optimally control in real time and in a coordinated fashion both continuous emissions monitoring (CEM) NO_x and ABS deposition location within the APH, avoiding NH_3 slip and minimizing APH heat rate penalty. The effectiveness of the ES adaptive controllers in keeping the system at an optimal operation point in presence of input disturbances and system changes (unit load, coal quality, firing system maintenance condition, SCR aging, etc.) is demonstrated through dynamic simulations.

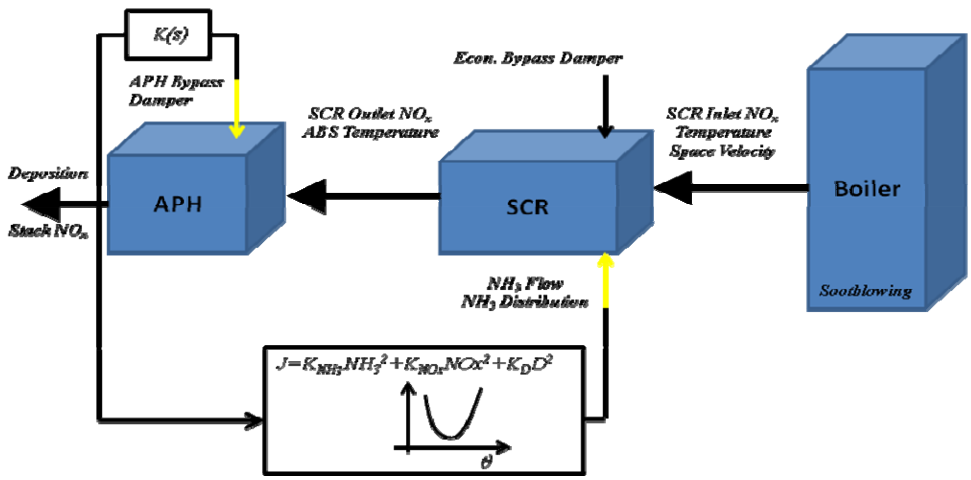

Fig. 13: SCR/APH adaptive control strategy.

4.1 Extremum Seeking

Extremum seeking control (Ariyur, 2003), a popular tool in control applications in the 1940-50's, has seen a resurgence in popularity as a *real time optimization* tool in different fields of engineering. In addition to being an optimization method, extremum seeking is a method of *adaptive control*, usable both for tuning set points in regulation/optimization problems and for tuning parameters of control laws. It is a *non-model based* method of adaptive control, and, as such, it solves, in a rigorous and practical way, some of the same problems as neural network and other intelligent control techniques. Aerospace and propulsion problems (formation flight (Binetti, 2002), combustion instabilities (Schneider, 2000; Banaszuk, 2004), flow control (Wang, 2000), compressor rotating stall (Ariyur, 2002)), automotive problems (anti-lock braking, engine mapping), bioreactors (Wang, 1999), and charged particle accelerators (Schuster, 2007) are among its applications. Extremum seeking is applicable in situations where there is a nonlinearity in the control problem, and the nonlinearity has a local minimum or a maximum. The nonlinearity may be in the plant, as a physical nonlinearity, possibly manifesting itself through an equilibrium map. Hence, one can use extremum seeking for tuning a set point to achieve an optimal value of the output. The parameter space can be multivariable. Without loss of generality, the static nonlinear block $J(\theta)$ is assumed to have a minimum J^* at $\theta=\theta^*$. The extremum seeking procedure guarantees that the estimation of θ, denoted as $\hat{\theta}$ in the figure, will converge to θ^*, minimizing J. A more detailed explanation of the fundaments of extremum seeking is presented in the Appendix.

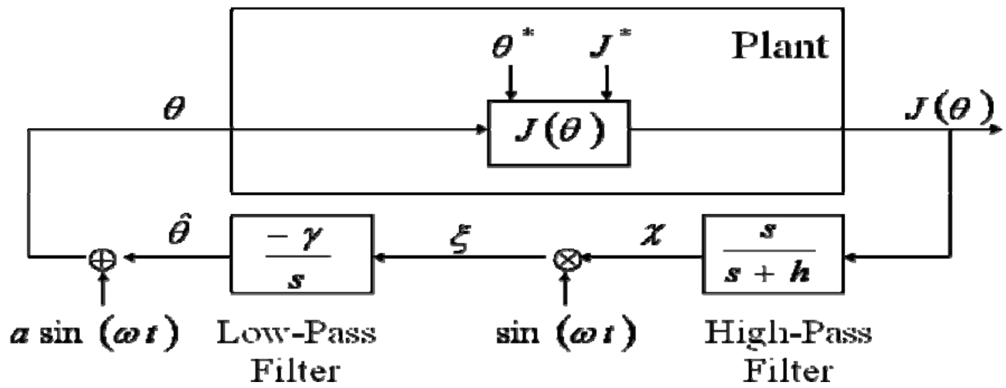

Fig. 14: Extremum Seeking algorithm.

4.2 SCR/APH Real-time Optimization

We propose in this section a combined extremum-seeking/PID control architecture as illustrated in Fig. 15. While the NH3 flow is directly controlled by an extremum-seeking controller, the APH bypass damper opening is controlled by a PID controller driven by the ABS deposition depth error. By defining the cost function as

$$J = K_{NOx} NOx\_CEM^2 + K_{NH3} NH3^2 + K_D D^2, \tag{6}$$

the extremum-seeking controller regulates the NH3 flow in order to minimize *NOx_CEM*, NH3 flow itself, and the APH bypass damper opening (D). The introduction of the bypass damper term in the cost function is a step forward in the efforts to coordinate the SCR and APH control loops. The user-defined weigh factors K_{NOx}, K_{NH3} and K_D regulates the tradeoff between *NOx_CEM* minimization and NH3/D minimization. Fig. 16 shows the simulation results. The level of NOx at the SCR inlet is varied as shown in Fig. 16 (a). It is possible to note that while the ABS deposition depth (Fig. 16 (f)) is regulated by the PID at a fixed set-point (2.5 ft), the level of CEM NOx (Fig. 16 (e)) has the freedom to fluctuate in order to minimize the cost function J shown in Fig. 16 (b). The minimizing variable is the NH3 flow rate shown in Fig. 16 (d). Note that the bypass damper opening shown in Fig. 16 (c) is kept at a relatively low value.

An alternative approach would control both the SCR and the APH systems by extremum seeking. The extremum seeking real-time optimizers could control the set-points for both *NOx_CEM* and ABS deposition depth instead of directly controlling the NH3 flow and the APH bypass damper opening. Conventional PID loops would be indeed in charge of controlling these variables based on the set-points received by the extremum seeking controllers. In this case the cost function would be defined as

$$J = K_{NOx} NOx\_CEM^2 + K_{NH3} NH3^2 + K_D D^2 + K_{APHD} APHD^2, \tag{7}$$

where the APH HR is assumed directly proportional to the measurable bypass damper opening (*APHD*). As stated by the cost function J, the control objective is the minimization of *NOx_CEM* and D using as little control effort (*NH3, APHD*) as possible.

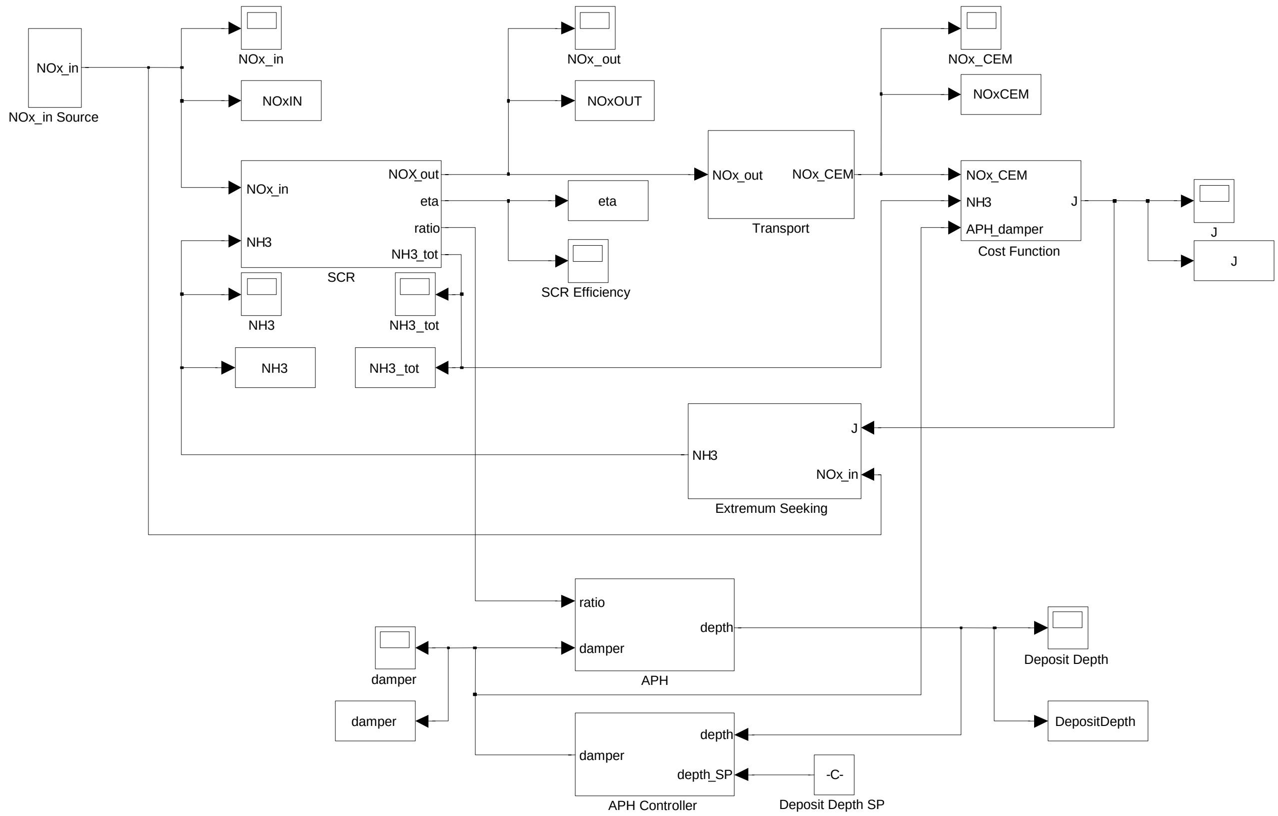

Fig. 15: Simulink Extemum Seeking SCR/APH control configuration.

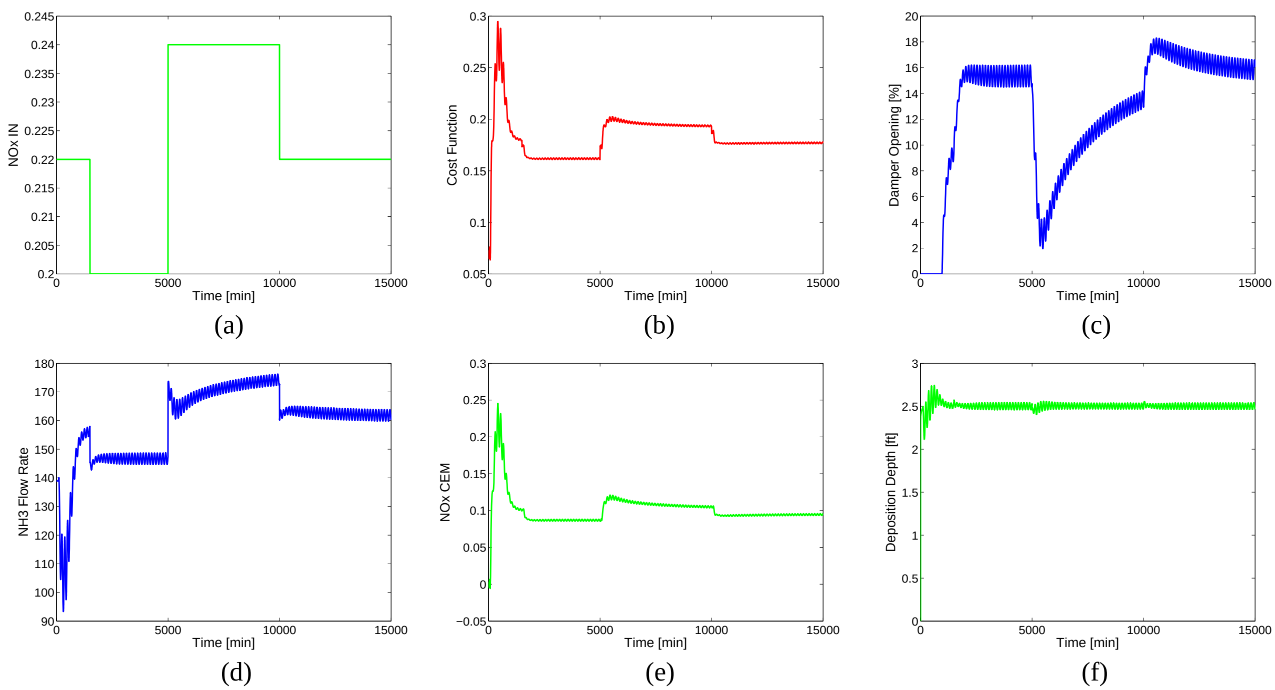

Fig. 16: Extremum seeking simulation results.

5. Conclusions and Future Work

With the ultimate goal of overcoming the deteriorating effects of time delays in the SCR control system, a multi-loop control strategy has been proposed. This multi-loop control approach has been complemented with a systematic method for optimal tuning of PID control gains. The control logic that is in use at Cayuga Unit 1 has been modified to include a scheme that incorporates the feedback measurements of Ammonium Bisulfate (ABS) fouling and Air Pre-Heater (APH) outlet temperature. This control system upgrade includes a control strategy provision for the APH bypass damper, which controls the ABS deposition location by controlling the average cold end APH temperature with the ultimate goal of minimizing APH plugging (ABS concentration). Simple dynamic models for the SCR system and APH system were identified from experimental data to capture the most dominant behavior of the system. It is important to emphasize that these models were developed with the unique goal of carrying out simulations for the proposed control schemes and were not used for control design.

A coordination of both the SCR and APH control systems has been proposed in order to enhance the overall performance of the system. This coordination is achieved through the relaxation of some of the control set-points. The simple idea behind this approach is that by relaxing some of the control set-points we may be able to gain more than what we loose. This ad hoc coordination approach leads to the definition of tradeoffs. These trade-offs are later optimally approached using extremum-seeking control techniques. Extremum seeking, a real-time optimization technique, is proposed as a robust adaptive control method that is able to optimally solve performance tradeoffs and to react to any input or plant change in order to keep the system at an optimal operation point. The non-model-based adaptive extremum-seeking controller is proposed to regulate the NH_3 flow to the SCR system and the APH bypass damper opening in order to optimally control in real time and in a coordinated fashion both continuous emissions monitoring (CEM) NO_x and ABS deposition location within the APH, avoiding NH_3 slip and minimizing APH heat rate penalty. Based on the results obtained during this project, the proposed approach has the potential for reduced stack NO_x emissions, reduced heat rate, reduced ammonia usage, reduced catalyst replacement, and savings in air pre-heater cleaning.

Recent work on static optimization of coal-based power plants has played a crucial role in improving overall efficiency. However, static optimization falls short in dealing with real-time scenario changes (i.e., cycling unit load, coal quality, firing system maintenance conditions, subsystem failures, plant aging, etc.). Taking into account all possible scenarios during an offline static optimization is simply unfeasible. When the plant conditions change in real-time and departs from the conditions considered during the offline static optimization, the optimal set-points are not longer optimal and need to be recomputed online. An extremum-seeking adaptive controller has the potential of overcoming this limitation. Our future work include the development of such controller for an integrated system composed by Boiler, Selective Catalytic Reduction (SCR) System and Air Preheater (APH) with the ultimate goal of optimally reducing the combined cost of unit NO_x compliance in real-time. The controller will regulate a set of boiler inputs (i.e., O_2, separated overfire (SOFA) registers, burner tilt, SOFA tilt, coal flows, etc.), NH_3 flow to the SCR system, economizer bypass damper opening and APH bypass damper opening in order to optimally control in real time continuous emissions monitoring (CEM) NO_x at the stack, SCR inlet NO_x, ammonium bisulfate (ABS) deposition location within the APH, ammonia reagent (NH_3) usage, NH_3 slip, and net unit heat rate.

Appendix

We give next an elementary intuitive explanation about how the scheme "works" (Ariyur, 2003). The perturbation signal $a\sin(\omega t)$ fed into the plant helps to get a measure of gradient information of the map $J(\theta)$. We posit $J(\theta)$ of the form:

$$J(\theta) = J^* + \frac{J''}{2}(\theta - \theta^*)^2$$

where $J''>0$. Any C^2 function $J(\theta)$ can be approximated locally in this way. The assumption $J''>0$ is made without loss of generality. If $J''<0$, we just replace $\gamma\,(\gamma>0)$ in Fig. 14 with $-\gamma$. The purpose of the algorithm is to make θ-θ^* as small as possible, so that the output $J(\theta)$ is driven to its minimum J^*. We start by noting that $\hat{\theta}$ in Fig. 14 denotes the estimate of the unknown optimal input θ^*. Let $\tilde{\theta} = \theta^* - \hat{\theta}$ denote the estimation error. Thus,

$$\theta(t)\text{-}\theta^* = \hat{\theta}(t) + a\sin(\omega t)\text{-}\theta^* = a\sin(\omega t)\text{-}\tilde{\theta}(t)$$

which, when substituted into the expression for $J(\theta)$, gives

$$J(t) \equiv J(\theta(t)) = J^* + \frac{J''}{2}\left(a\sin(\omega t) - \tilde{\theta}(t)\right)^2$$

Expanding this expression further, and applying the basic trigonometric identity $2\sin^2(\omega t) = 1 - \cos(2\omega t)$, one gets

$$J(t) \equiv J(\theta(t)) = J^* + \frac{a^2 J''}{4} + \frac{J''}{2}\tilde{\theta}^2(t) - aJ''\tilde{\theta}(t)\sin(\omega t) - \frac{a^2 J''}{4}\cos(2\omega t)$$

The washout (high pass) filter $s/(s+h)$, with $h>0$, applied to the output, serves to remove the DC components, namely,

$$\chi(t) = \frac{J''}{2}\tilde{\theta}^2(t) - aJ''\tilde{\theta}(t)\sin(\omega t) - \frac{a^2 J''}{4}\cos(2\omega t)$$

This signal is then "demodulated" by multiplication with $\sin(\omega t)$, giving

$$\xi(t) = \frac{J''}{2}\tilde{\theta}^2(t)\sin(\omega t) - aJ''\tilde{\theta}(t)\sin^2(\omega t) - \frac{a^2 J''}{4}\cos(2\omega t)\sin(\omega t)$$

Applying again $2\sin^2(\omega t) = 1 - \cos(2\omega t)$, as well as the identity $2\cos(2\omega t)\sin(\omega t) = \sin(3\omega t) - \sin(\omega t)$, we arrive at

$$\xi(t) = -\frac{aJ''}{2}\tilde{\theta}(t) + \frac{aJ''}{2}\tilde{\theta}(t)\cos(2\omega t) + \frac{a^2 J''}{8}(\sin(\omega t) - \sin(3\omega t)) + \frac{J''}{2}\tilde{\theta}^2(t)\sin(\omega t)$$

First, we neglect the last term because it is quadratic in $\tilde{\theta}$ and we are interested only in local analysis. Second, when we pass the signal through the low-pass filter (integrator) $-\gamma / s$, the high frequency components (last two terms) get greatly attenuated. Thus, we neglect them, getting

$$\hat{\theta}(t) = \frac{\gamma}{s}\frac{aJ''}{2}\tilde{\theta}(t) \Leftrightarrow \dot{\hat{\theta}}(t) = \frac{\gamma a J''}{2}\tilde{\theta}(t)$$

Noting that, because θ^* is constant, $\dot{\hat{\theta}}(t) = -\dot{\tilde{\theta}}(t)$, we can write

$$\dot{\tilde{\theta}}(t) = -\gamma\frac{aJ''}{2}\tilde{\theta}(t)$$

Since $\gamma a J'' > 0$, this is a stable system. Thus, we conclude that $\tilde{\theta} \to 0$, or, in terms of the original problem, $\hat{\theta}$ converges to within a small distance of θ^*.

References

Ariyur, K., and Krstic, M.,"Slope seeking and application to compressor instability control", *2002 IEEE Conference on Decision and Control*, Las Vegas, Nevada, pp. 3690–3697, Dec. 2002.

Ariyur, K., and Krstic, M., *Real-Time Optimization by Extremum Seeking Feedback*, Wiley, 2003.

Banaszuk, A., Ariyur, K., Krstic, M., Jacobson, C.A., "An adaptive algorithm for control of combustion instability," *Automatica* 40 (2004) 1965 – 1972.

Binetti, P., Ariyur, K., Krstic, M., Bernelli, F., "Control of formation flight via extremum seeking", *2002 American Control Conference*, Anchorage, Alaska, pp. 2848–2853, May 2002.

Cichanowicz, E., and Smith, L., "SCR performance analysis hints at difficulty in achieving high NOx removal targets," Power Eng 2002;106:82–90.

Romero, C., and Sarunac, N., "Field results from application of Boiler OP to utility boilers," *43rd Annual ISA POWID Controls and Instrumentation Conference*, San Antonio, TX, June 4–9; 2000.

Schneider, G., Ariyur, K., Krstic, M., "Tuning of a combustion controller by extremum seeking: A simulation study," *Conf. on Decision and Control*, Sydney, Australia, pp.5219–5223, Dec. 2000.

Schuster, E., Xu, C., Torres, E., Morinaga, E., Allen, C.K., and Krstic, M., "Beam Matching Adaptive Control via Extremum Seeking," *Nuclear Instruments and Methods in Physics Research A*, v 581, n 3, Nov. 2007, p 799–815..

Si, F., Romero, C.E. , Yao, Z., Schuster, E., Xu, Z., Morey, R.L. , Liebowitz, B.N., "Optimization of Coal-fired Boiler SCRs Based on Modified Support Vector Machine Models and Genetic Algorithms," *Fuel*, in press.

Wang, H.-H., Krstic, M., and Bastin, G., "Optimizing bioreactors by extremum seeking," *International Journal of Adaptive Control and Signal Processing*, vol. 13, pp. 651–659, 1999.

Wang, H.-H., Yeung, S., Krstic, M., "Experimental application of extremum seeking on an axial-flow compressor," *IEEE Trans. on Control Systems Technology,* vol. 8, pp. 300–309, 2000.